Brazilian Journal
of Chemical
Engineering

ISSN 0104-6632
Printed in Brazil

Vol. 21, No. 04, pp. 629 - 640, October - December 2004

USING PERVAPORATION DATA IN THE CALCULATION OF VAPOUR PERMEATION HOLLOW-FIBRE MODULES FOR AROMA RECOVERY

C. P. Ribeiro Jr. and C. P. Borges*

Programa de Engenharia Química, COPPE , Universidade Federal do
Rio de Janeiro, UFRJ, Phone (21) 2562-8351, Fax (21) 2562-8300,
Cx P. 68502, CEP: 21945-970, Rio de Janeiro - RJ
E-mail: cristiano@peq.coppe.ufrj.br

(Received: January 3, 2003 ; Accepted: July 1, 2004)

Abstract - Taking into account the close similarity between pervaporation and vapour permeation techniques, a method for employing pervaporation flux data in the modelling of vapour permeation modules is proposed. It is based on the use of fugacity gradients across the membrane, instead of concentration ones, as the driving force for mass transfer. This procedure is interesting, for instance, in the case of aroma recovery systems, for which there is much more experimental data on pervaporation available in the literature than on vapour permeation. In order to illustrate the application of this method, pervaporation experiments for an isotropic PDMS membrane were conducted with aqueous solutions of ethyl acetate (113-2474 mg/L), and the results obtained were used to enable simulation of different vapour permeation hollow-fibre modules for recovering ethyl acetate from diluted air streams.
Keywords: pervaporation, vapour permeation, aroma, VOC, fruit juices.

INTRODUCTION

Pervaporation and vapour permeation are similar membrane-based separation processes whose basic difference lies in the physical state of the feed stream, which is a liquid in the former case and a vapour in the latter. In both processes a gaseous permeate is obtained from the fluid feed stream and a non-porous membrane is employed in the separation.

The selective permeation of different components through a membrane is essentially a mass-transfer process; therefore a chemical potential gradient constitutes its driving force (Cussler, 1984). Taking into account the fact that at equilibrium the chemical potential of each component must be the same in all phases, it is easy to understand the similarity between pervaporation and vapour permeation. In pervaporation, the chemical potential gradient results from a vapour pressure difference across the membrane, whereas in vapour permeation a partial pressure difference is responsible for generating the chemical potential gradient. Whichever the process, the permeate side is kept under high vacuum in order to maximise the driving force for mass transport across the membrane.

Compared to other membrane processes, such as ultrafiltration and reverse osmosis, pervaporation and vapour permeation generally have low fluxes (< 10 kg h^{-1} m^{-2}). Nonetheless, their selectivity can be extremely high, often exceeding 1000 (Fleming and Slater, 1992). These aspects explain why these techniques are applied when the removal of dilute components from a solution is desired.

*To whom correspondence should be addressed

The recovery of aroma compounds by pervaporation during fruit juice processing, in particular, has drawn considerable attention (Karlsson and Trägardh, 1993). In order to reduce transportation and packaging costs, fruit juices are concentrated in multiple-effect evaporators under vacuum (Ramteke et al., 1993), and in this step the so-called aroma compounds are transferred to the vapour phase due to their high volatility in aqueous solutions. These compounds are responsible for the specific odour and flavour of a given juice, and hence must be recovered and then added back to the concentrated juice before packing.

Many experimental studies have been conducted on the pervaporation of aroma compounds, as shown by Shepherd (2000) in a recent review. One major drawback of pervaporation in this application seems to be the severe concentration polarisation effect associated with the boundary layer resistance to mass transfer on the feed side, which reduces both flux and selectivity. Its occurrence in aroma recovery experiments has already been verified, for instance, by Bengtsson et al. (1993), Olsson and Trägardh (1999) and Sampranpiboon et al. (2000).

Concentration polarisation, however, is much less likely in vapour permeation owing to the lower viscosity of gases in comparison to liquids, which ensures a higher Reynolds number on the feed side for a given mass flow rate, and hence a higher degree of turbulence, reducing the thickness of the mass-transfer boundary layer. Furthermore, vapour permeation requires no liquid-vapour phase change to occur while the component goes from the feed to the permeate side, and hence the problems related to supplying the enthalpy of evaporation in the separation process, which can lead to significant drops in the flux of a pervaporation unit (Karlsson and Trägardh, 1996), are avoided. In view of these advantages, vapour permeation could offer an interesting alternative for recovering aroma compounds straight from the gaseous streams exiting evaporators.

Although a substantial number of studies has already been published demonstrating the efficacy of vapour permeation in the recovery of volatile organic compounds (VOC's) from diluted gaseous streams (Paul et al., 1988; Kimmerle et al., 1988; Ohlrogge et al., 1990; Blume et al., 1991; Sander and Janssen, 1991; Lahiere et al., 1993; Deng et al., 1995; Yeom et al., 2002), the amount of data on vapour permeation of aroma compounds in the literature is rather limited. Apparently, only two different substances have been considered so far, namely ethyl acetate (Leemann et al., 1996; Gales et al., 2002) and benzaldehyde (Fouda et al., 1993), whereas for pervaporation almost 60 different aroma compounds have already been examined (Baudot et al., 1999). In this work, bearing in mind the close relation between these two membranes techniques, a method for employing pervaporation data in the modelling of vapour permeation modules is proposed. In order to illustrate its application, pervaporation experiments for the recovery of a typical aroma compound were performed and the results obtained were applied in the simulation of different vapour permeation hollow-fibre modules.

MATHEMATICAL FORMULATION

Flux Equations

Since the driving force for mass transfer is a chemical potential gradient and the equality of chemical potentials for each species in all phases constitutes the thermodynamical criterion of phase equilibrium, pervaporation and vapour permeation must provide the same results when respectively applied to a liquid solution and to the vapour at equilibrium with it. This theoretical prediction was recently confirmed experimentally by Uchytil and Petrickovic (2002). Therefore, permeability data determined in pervaporation tests may be utilised for predicting the performance of vapour permeation units and vice versa.

Traditionally, when concentration polarisation can be neglected, permeability (P_m^i) is calculated by expressing the flux across the membrane (J_i) as a function of the species concentration in the feed and permeate phases, x_i^F and x_i^P:

$$J_i = \frac{P_m^i}{l}\left(x_i^F - x_i^P\right) \tag{1}$$

where l is the membrane thickness. However, the use of permeability values determined in pervaporation tests by eq. (1) will provide erroneous results for vapour permeation fluxes since the equality of concentrations does not mean equality of chemical potentials, specially for aqueous solutions of hydrophobic organic substances like aroma compounds. Consequently, in order to enable the calculation of a vapour permeation module from pervaporation data, an alternative expression for mass fluxes across the membrane has to be employed.

In terms of the real driving force for the

pervaporation and vapour permeation processes, the flux, which is assumed to be unidirectional and not affected by coupling, is given by the following transport relation:

$$J_i = -L_i \frac{d\mu_i}{dz} \tag{2}$$

where L_i is a phenomenological coefficient to be experimentally determined and μ_i is the chemical potential of species i.

For an isothermal process, the chemical potential of species i is expressed as

$$d\mu_i = RTd\left(\ln \hat{f}_i\right) \tag{3}$$

where $\hat{f}_i$ is the fugacity of component i in solution.

Considering isothermal vapour permeation and pervaporation processes, eq. (3) is substituted into eq. (2) to give

$$J_i = -RTL_i \frac{d\left(\ln \hat{f}_i\right)}{dz} \tag{4}$$

Assuming a linear fugacity profile across the membrane, eq. (4) can be approximated by the following expression:

$$J_i = \frac{\Lambda_i}{l}\left(\hat{f}_i' - \hat{f}_i''\right) \tag{5}$$

in which $\hat{f}_i'$ and $\hat{f}_i''$ are the fugacities of species i in the membrane for the feed/membrane and membrane/permeate interfaces, respectively, and Λ_i is a new phenomenological coefficient defined as

$$\Lambda_i \equiv -\frac{RTL_i}{\left\langle \hat{f}_i \right\rangle} \tag{6}$$

where $\left\langle \hat{f}_i \right\rangle$ represents an averaged fugacity of i across the membrane.

From eq. (3), it is clear that the equality of chemical potentials implies the equality of fugacities. Thus, using the interfacial equilibrium hypothesis of the sorption-diffusion model (Wijmans and Baker, 1995), which is the one used for describing the permeation of species in non-porous membranes, eq. (5) can be rewritten as

$$J_i = \frac{\Lambda_i}{l}\left(\hat{f}_i^F - \hat{f}_i^P\right) \tag{7}$$

where $\hat{f}_i^F$ and $\hat{f}_i^P$ are the fugacities of component i in the feed and permeate phases, respectively, assuming the concentration polarisation effect to be negligible.

For a given pressure on the permeate side, eq. (7) predicts the same flux J_i for a species that, on the feed side, is either in a liquid solution or in the vapour phase at equilibrium with this liquid and thereby establishes a direct relation between pervaporation and vapour permeation. The transport characteristics of the membrane, which of course do not depend upon the physical state of the feed, are described by parameter Λ_i. All non-ideality effects of the feed solutions are included in the fugacity of component i. The great advantage of eq. (7) over the traditional relation, eq. (1), is exactly this separation between the contributions related to the membrane and the feed non-ideality, which are lumped together in parameter P_m^i of eq. (1).

In pervaporation, as the feed is a liquid solution, the fugacity of species i is given by

$$\hat{f}_i^L = \gamma_i x_i \phi_i^{sat} P_i^{sat} \exp\left[\frac{\int_{P_i^{sat}}^{P} V_i dP}{RT}\right] \tag{8}$$

where γ_i is the activity coefficient of species i in solution, x_i is the molar fraction of i in the solution, ϕ_i^{sat} is the fugacity coefficient of saturated liquid, P_i^{sat} is the vapour pressure of i at the solution temperature and V_i is the liquid molar volume of species i. The value of γ_i is calculated from excess Gibbs energy models, such as NRTL or UNIQUAC, whereas ϕ_i^{sat} can be determined, for instance, from an equation of state.

Neglecting the variation of liquid-phase molar volume with pressure, which is quite small for temperatures well below the critical one (Smith and Van Ness, 1987), and evaluating V_i at the saturation condition, eq. (8) is simplified to

$$\hat{f}_i^L = \gamma_i x_i \phi_i^{sat} P_i^{sat} \exp\left[\frac{V_i^{sat}\left(P - P_i^{sat}\right)}{RT}\right] \tag{9}$$

where the exponential term is known as the Poynting

factor.

On the permeate side, as the components are in the vapour phase, their fugacities in solution are expressed as

$$\hat{f}_i^V = \hat{\phi}_i x_i P \tag{10}$$

where $\hat{\phi}_i$ is the fugacity coefficient of i in solution, which can be estimated from an equation of state.

Upon substituting eqs. (10) and (9) into eq. (7), one obtains the relation for the molar flux of species i in pervaporation:

$$J_i^{PV} = \frac{\Lambda_i}{l}\left\{\begin{array}{l}\gamma_i^F x_i^F \phi_i^{sat} P_i^{sat} \\ \exp\left[\dfrac{V_i^{sat}\left(P^F - P_i^{sat}\right)}{RT}\right] - \hat{\phi}_i^P x_i^P P^P\end{array}\right\} \tag{11}$$

In vapour permeation, as feed and permeate are gaseous solutions, eq. (10) is valid for both, so that the molar flux is written as

$$J_i^{VP} = \frac{\Lambda_i}{l}\left(\hat{\phi}_i^F x_i^F P^F - \hat{\phi}_i^P x_i^P P^P\right) \tag{12}$$

Eqs. (11) and (12) are quite general and may be considerably simplified depending upon the process operating conditions. Since the operating pressure on the feed side is low for both pervaporation and vapour permeation, the ideal gas hypothesis is a good approximation, so the fugacity coefficients of species i pure and in solution may be regarded as equal to one. Moreover, the Poynting factor is only significant for extremely high pressure differences. For water, for instance, a pressure difference of 10 atm, which is much bigger than those observed in pervaporation, results in a Poynting factor of only 1.007. As a result, this term can also be considered equal to one. In addition, on account of the high vacuum on the permeate side, it is assumed that P^P is zero. With these assumptions, eqs. (11) and (12) are rewritten as

$$J_i^{PV} = \frac{\Lambda_i}{l}\gamma_i^F x_i^F P_i^{sat} \tag{13}$$

$$J_i^{VP} = \frac{\Lambda_i}{l} x_i^F P^F \tag{14}$$

The activity coefficient γ_i is a function of the temperature and the composition of the solution. Nevertheless, for highly diluted systems, like the ones dealt with in aroma recovery, the interactions between different solute molecules and between the molecules of a given species may be ignored, so the composition dependence vanishes and the solute flux can be calculated by means of the so-called infinite dilution coefficient, γ_i^∞, which depends only on temperature:

$$J_i^{PV} = \frac{\Lambda_i}{l}\gamma_i^\infty x_i^F P_i^{sat} \tag{15}$$

According to Bomben et al. (1973), the infinite dilution approximation can be applied for aroma solutions provided that the total mole fraction of organic compounds does not exceed approximately 10^{-3}.

Hollow-Fibre Module Simulation

In order to simulate the operation of a vapour permeation hollow-fibre module, apart from eq. (14), the total and component mass balances are required. Assuming a uniform distribution of the feed stream between the n_f fibres which comprise the permeation module, analysis of only one fibre enables simulation of the entire equipment. If F_T is the total molar flow rate in the module, J is the total permeate flux in a single fibre and the hypothesis of plug flow is valid, the global mass balance for the module is given by

$$\frac{dF_T}{dz} = -\pi n_f d_f J \tag{16}$$

where d_f is the diameter of the fibre, either internal or external, depending on whether the feed stream flows inside or outside the fibres, respectively.

For a gaseous mixture containing NC components, the total permeate flux equals the sum of the flux of each species. Expressing the individual fluxes by eq. (14), one obtains the following relation for the variation of total flow rate along the fibre:

$$\frac{dF_T}{dz} = -\pi n_f d_f \left(\sum_{i=1}^{NC} \frac{\Lambda_i}{l} x_i P\right) \tag{17}$$

The mass balance for species i in the permeation module is

$$\frac{d}{dz}\left(F_T x_i\right) = -\pi n_f d_f J_i \tag{18}$$

which is equivalent to

$$F_T \frac{dx_i}{dz} + x_i \frac{dF_T}{dz} = -\pi n_f d_f J_i \tag{19}$$

Substitution of eqs. (17) and (14) into (19) gives

$$\frac{dx_i}{dz} = -\frac{\pi n_f d_f}{lF_T} x_i P\left(\Lambda_i - \sum_{j=1}^{NC} \Lambda_j x_j\right) \tag{20}$$

The variation of pressure in the module derives from the friction with the membrane walls and from the diminution in total number of moles due to permeation. However, for na aroma recovery system, the feed stream is highly diluted in the components which preferably permeate through the membrane, and hence the percentage difference between the inlet and outlet molar flow rates is small. As a result, in this work, only the friction effect was taken into account, and as previously done by Bruining (1989) and Gales et al. (2002), it was estimated using the Hagen-Poiseuille equation (Bird et al., 1960):

$$\frac{dP}{dz} = -\frac{128\eta F_T}{\pi n_f \rho \ d_f^4} \tag{21}$$

The system of NC + 1 first-order, ordinary differential equations comprised of eqs. (17), (20) and (21) enables calculation of the retentate composition for a given vapour permeation module. The initial conditions for this system of equations are

$$F_T = F_T^F \quad \text{at} \quad z = 0 \tag{22a}$$

$$x_i = x_i^F \quad \text{at} \quad z = 0 \tag{22b}$$

$$P = P^F \quad \text{at} \quad z = 0 \tag{22c}$$

Analysis of eq. (22c) indicates that the pressure drop associated with the entrance effects in the module has been neglected.

In this work, the system of differential equations was integrated using the fourth-order Runge-Kutta method. In order to avoid normalisation of molar fractions during integration, eq. (20) was written for NC – 1 components with the molar fraction of component NC calculated by the relation:

$$x_{NC} = 1 - \sum_{i=1}^{NC-1} x_i \tag{23}$$

For simulation of the module, its total number of fibres as well as their diameter and length has to be specified. Its performance can be assessed, for instance, by means of the degree of recovery, DR, defined by the following expression:

$$DR_i = \frac{x_i^F - x_i^R}{x_i^F} \tag{24}$$

in which x_i^R refers to the mole fraction of component i in the retentate. From eq. (24), it is clear that $0 \le DR_i \le 1$. The closer to one the value of DR_i, the lower the amount of species i lost after the treatment of the feed stream in the membrane module.

EXPERIMENTAL

Pervaporation tests were performed with dense, isotropic PDMS membranes provided by Multiplast®. These fibres had an inner diameter of 0.5 mm and their walls were 0.25 mm thick. The chosen solute was ethyl acetate, a typical aroma compound for many fruit juices.

The experimental set-up used for conducting the pervaporation experiments is shown in Figure 1. The feed was kept at constant temperature (298 K) and circulated through the membrane module by a gear pump. The module contained 9 PDMS fibres and had a total permeation area of 5.65×10^{-3} m^2, and the feed flowed on shell side, whose external diameter was 0.0165 m. The permeate pressure was kept lower than 3 mmHg. After a stabilisation period of 2 h, the permeate fluxes and separation factors were measured for different solute concentrations and feed flow rates. The permeate was cooled with liquid nitrogen and weighed at room temperature. The feed and permeate were sampled and analysed by refractometry (Shimadzu refractometer, model RID-10A)

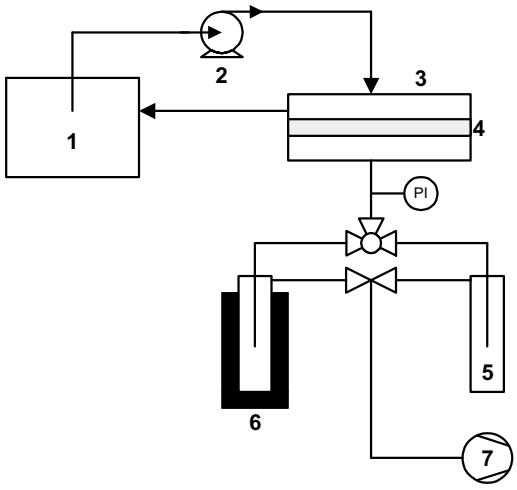

1) feed tank
2) gear pump
3) permeation module
4) membrane
5) crystalliser
6) liquid nitrogen
7) vacuum pump

Figure 1: Experimental set-up for pervaporation tests.

RESULTS AND DISCUSSION

Pervaporation Tests

The ethyl acetate molar fraction in the feed stream was varied from 2.3×10^{-5} to 5.1×10^{-4} (113 to 2474 mg/L), using three different feed flow rates. The experimental results obtained for the pervaporation fluxes in the isotropic PDMS membrane are portrayed in Figures 2 and 3.

For ethyl acetate, an analysis of Figure 2 reveals first a linear relationship between flux and solute concentration, which indicates a negligible membrane swelling for the operating conditions investigated. This observation is in agreement with the results presented by Clément et al. (1992), who studied the pervaporation of aqueous solutions of ethyl acetate with composite PDMS membranes and noticed that the swelling was only significant for solute concentrations bigger than 5.0 %wt.

For a given ethyl acetate concentration, the data in Figure 1 indicate that the feed flow rate has no substantial effect on the ester flux. Since the feed flow rate influences the boundary layer resistance to mass transfer on the feed side, it can be concluded that, for the module studied in this work, this resistance is much smaller than the one associated with the membrane, or in other words, concentration polarisation does not play an important role. This situation is seldom verified for aroma pervaporation, as previously discussed, but can be justified owing to the fact that the wall of the dense isotropic membrane employed is considerably thicker than those of the composite membranes used in most of the studies reported in the literature. It should be emphasised that, of all the esters that can be found in the aroma complex of fruit juices, ethyl acetate is the least hydrophobic, and accordingly the one which has the lowest selectivity for pervaporation with organophilic membranes. As shown by Feng and Huang (1994), the concentration polarisation effect is intensified with an increase in membrane selectivity. For ethyl butanoate solutions, Shepherd et al. (2002) observed that, even for the dense isotropic PDMS membrane considered in this work, concentration polarisation poses a problem in separation by pervaporation.

In agreement with previous findings of Clément et al. (1992) and Pereira et al. (2002), the data on water in Figure 3 do not show any systematic pattern of variation as the ethyl acetate concentration is changed, being scattered around a mean value that did not depend on the feed flow rate. Considering all points in Figure 3 as individual estimates from the same value, a mean water flux of (7.4 ± 1.2) g h^{-1} m^{-2} was computed for the PDMS isotropic membrane used. The solid line drawn in Figure 3 corresponds to this mean value.

On account of the low ester concentrations utilised in the tests, the driving force for water transport does not vary substantially. Nonetheless, the water flux could still be a function of ethyl acetate concentration, should there be flux coupling between these two species. The results obtained thus demonstrate that, for the operating conditions analysed, the two compounds permeate independently across the membrane.

As the water flux does not vary, the linear increase in the ethyl acetate flux with its concentration on the feed side implies a similar

variation pattern for the concentration of this ester on the permeate side, which is confirmed by the experimental data shown in Figure 4.

Aiming at the estimation of parameter Λ_i/l for ethyl acetate in the PDMS membrane, the ester fugacity in the feed stream was calculated for each experimental condition, using the infinite dilution activity coefficient and the vapour pressure relation reported respectively by Sancho et al. (1997) and Reid et al. (1987). The variation of ethyl acetate flux as a function of fugacity is shown in Figure 5; since there is no effect of feed flow rate, the differentiation of the experimental points according to this variable was removed. It is clear that the flux increases linearly with the fugacity of solute in the feed stream, indicating the adequacy of eq. (13) for this system. Performing a linear regression of the data presented in Figure 5 and setting the linear coefficient of the adjusted line to zero, a value of $(1.53 \pm 0.06) \times 10^{-4}$ mol h^{-1} Pa^{-1} m^{-2} was obtained for Λ_i/l. The adjusted line, with a correlation coefficient of 0.96, is also shown in Figure 5.

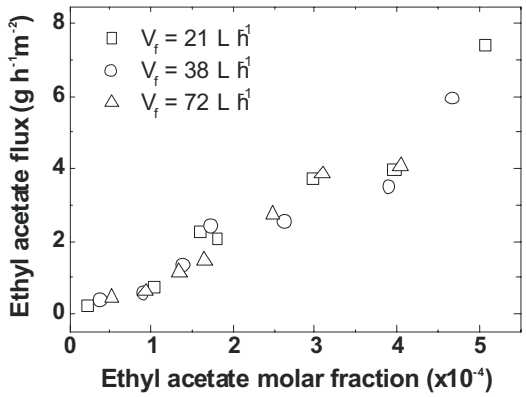

Figure 2: Pervaporation fluxes of ethyl acetate as a function of its concentration in the feed stream for three different feed flow rates.

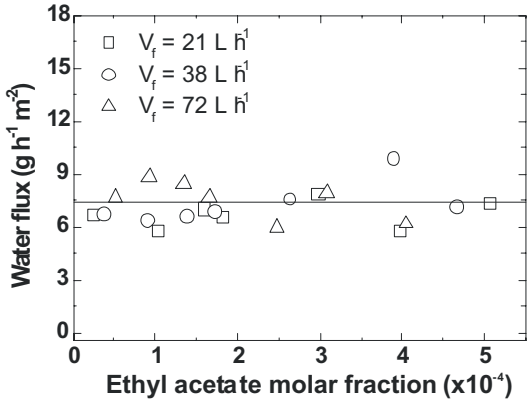

Figure 3: Pervaporation fluxes of water as a function of ethyl acetate concentration in the feed stream for three different feed flow rates.

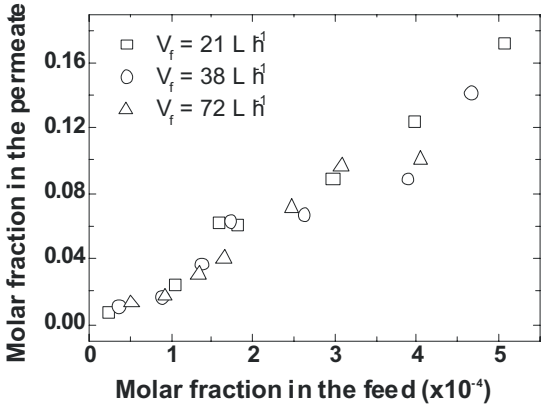

Figure 4: Concentration of ethyl acetate in the permeate as a function of the concentration of this ester in the feed stream for three different feed flow rates.

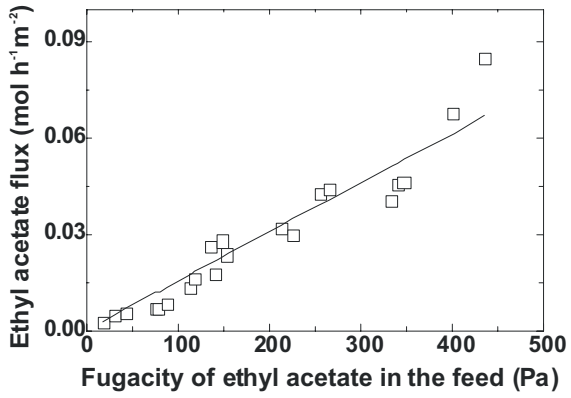

Figure 5: Ethyl acetate flux for the PDMS membrane as a function of the fugacity of this component in the feed stream: points – experimental data; line – adjusted model.

Simulation of Vapour Permeation Modules

Once the parameter Λ_i/l for ethyl acetate has been calculated, it would be desirable to apply eqs. (17) and (20)-(22c) to predict the performance of a vapour permeation hollow-fibre module and compare the calculated ester flux with the experimental one. However, neither of the experimental data sets found in the literature for vapour permeation of ethyl acetate in PDMS could be used in this work. For the first data set, presented by Leemann et al. (1996), the thickness of the PDMS layer in the composite membrane utilised was not specified, whereas, for the second data set, published by Gales et al. (2002), not only the PDMS selective layer but also the PEI support layer of the composite membrane showed significant mass transport resistance.

Consequently, it was decided to illustrate the applicability of the mathematical model by using it in the evaluation of the most appropriate module configuration for a given separation. The main parameter in every permeation module is the membrane area, which, in the hollow-fibre units, can be varied either with the number or the length of fibres. Therefore, the same permeation area can be obtained with different module configurations. A simulation model such as the one described in section 2.2 provides the means for assessing the performance of each configuration and choosing the one to be used in the module.

As an example, a feed stream at 2.02×10^5 Pa and 298 K containing 1000 mg/L of ethyl acetate dissolved in air is to be treated in a vapour permeation module. Using the PDMS fibres studied in the pervaporation tests and considering that the permeate flows on the shell side of the module, a series of simulations was performed to determine the separation capacity of different modules by varying the number of fibres, the length of the fibres and the feed flow rate. The simulation results for the degree of recovery of ethyl acetate and the pressure drop in the modules are shown in Figures 6 and 7, respectively. It should be emphasised that, although the total flow rate to be treated is fixed in a real problem, the flow rate fed to each module can be varied due to the possibility of operation with a parallel arrangement.

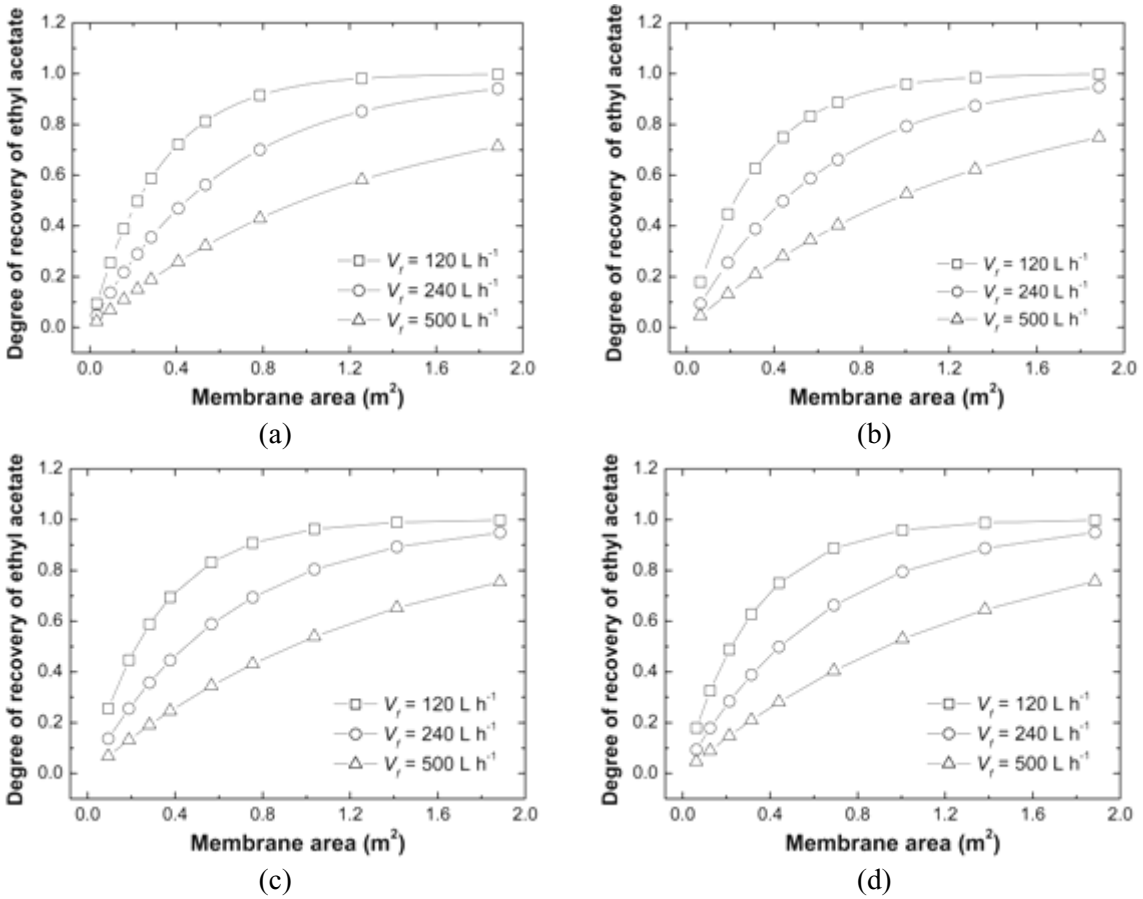

Figure 6: Simulation results for the variation of the degree of recovery of ethyl acetate as a function of the membrane area in vapour permeation modules, considering three feed flow rates and four different numbers of fibres in the modules: (a) 200; (b) 400; (c) 600; (d) 800.

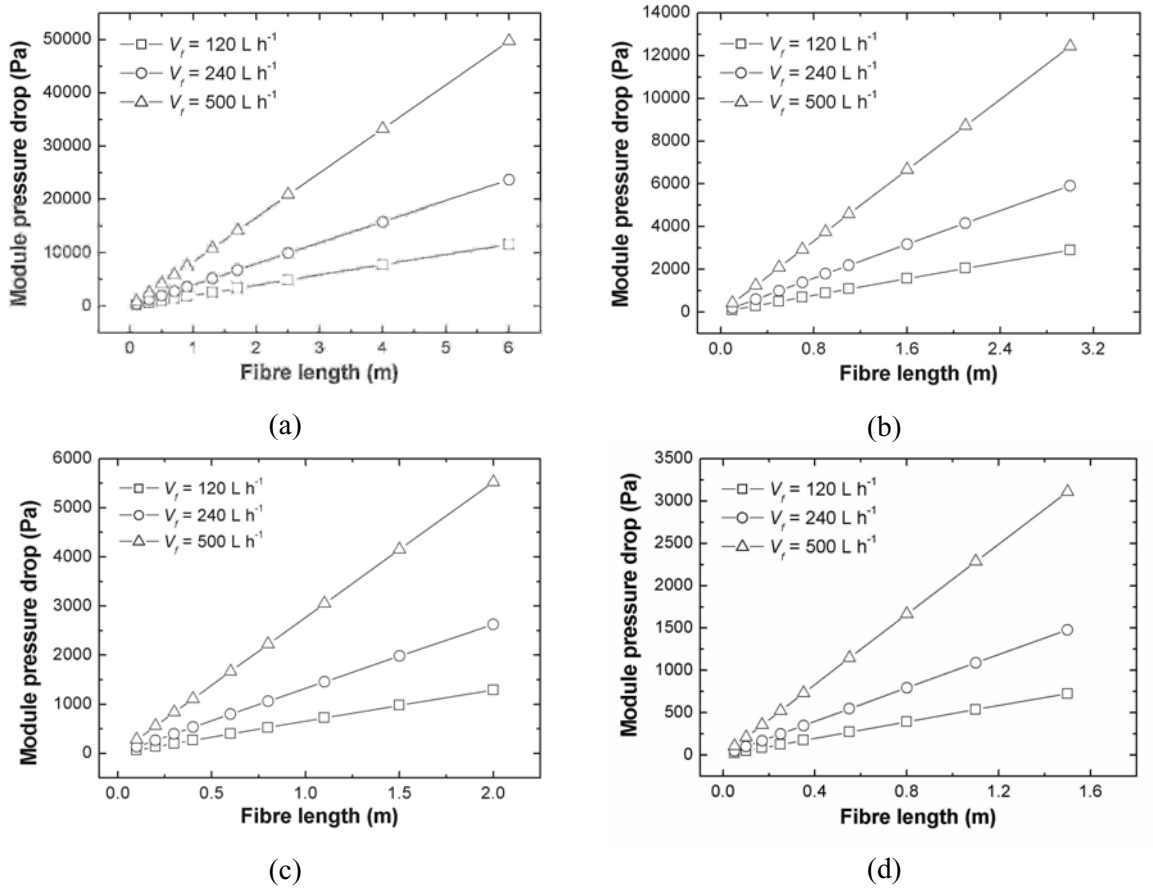

Figure 7: Simulation results for the variation of pressure drop on the feed side as a function of fibre length in vapour permeation modules, considering three feed flow rates and four different numbers of fibres in the modules: (a) 200; (b) 400; (c) 600; (d) 800.

An analysis of Figure 6 reveals that the degree of recovery grows asymptotically with the permeation area. Thus, the higher the degree of recovery, the larger the percentage increase in the area required to bring about the same percentage variation in DR. In the example considered, for a feed flow rate of 240 L/h per module in units with 800 fibres each, for instance, when DR is 0.32, a 10% increase in this value implies a permeation area 1.13 times larger, whereas, when DR is 0.90, the same 10% increase in DR requires a two-fold augmentation in the membrane area. When DR rises, the solute concentration on the feed side of the membrane falls accordingly, and hence the driving force for the mass transport of this solute across the membrane diminishes, which leads to the requirement of a larger area to achieve the same flux. These results demonstrate that construction of a module with a DR value very close to one, though desired from a theoretical point of view, is not economically viable on account of the considerable membrane area required, so a compromise between acceptable values of both costs and degree of recovery has to be reached.

Another point highlighted by the simulation results in Figure 6 is the effect of the feed flow rate. For a given membrane area, the degree of recovery in the module increases as the feed flow rate diminishes. Since plug flow is assumed in the simulation model, an increase in the flow rate produces a reduction in the residence time of the gaseous stream in the module, so, for the same flux J_i, the amount of species i which actually permeates across the membrane is lower, resulting in a smaller degree of recovery. This outcome points to the advantage of operating with a parallel arrangement of modules. There is, of course, a minimum limit for the flow rate to be fed to the modules, since concentration polarisation, which was not taken into account in the present model, may become significant if too low a flow rate is used, in which case the separation performance of the module would be seriously damaged.

For pressure drop on the feed side, the data in

Figure 7 show that modules with the same permeation area can have quite different results. Regardless of both the feed flow rate and the number of fibres, the pressure drop in the module increases with fibre length in a linear fashion. Since the difference between the partial pressures of species i on the feed and the permeate side of the membrane actually constitutes the driving force for permeation, it is clear that the pressure drop in the module ought to be minimised. For a fixed length of any number of fibres, the pressure drop increases with the feed flow rate, an effect which stems from the increase in the friction with the membrane walls as the flow velocity grows. For the same feed flow rate, a greater number of fibres implies a lower flow velocity per fibre and, as a consequence, an inferior pressure drop per fibre length is obtained, as one can see by comparing Figures 7a to 7d. These results indicate that, as far as pressure drop is concerned, for obtaining a given membrane area, it is interesting to work with a greater number of fibres and shorter lengths.

CONCLUSIONS

A method for predicting vapour permeation fluxes from pervaporation data was developed; its main feature is the utilisation of fugacity gradients across the membrane as the driving force for mass transfer. This method is particularly advantageous for systems such as the ones found in aroma recovery, for which there is a considerable amount of experimental data on pervaporation available in the literature, but little on vapour permeation.

The proposed method was applied for ethyl acetate, a typical aroma compound, in a PDMS hollow-fibre membrane. With the aid of results from pervaporation tests, different vapour permeation modules were simulated. It was shown that the degree of recovery increases asymptotically with membrane area. Furthermore, it was verified that, for a given permeation area, the pressure drop in the module falls as a greater number of fibres with shorter lengths is used.

NOMENCLATURE

d_f	fibre diameter,	m
DR	degree of recovery, dimensionless	(-)
F_T	total flow rate in the module,	mol s^{-1}
$\hat{f}$	fugacity in solution,	Pa
$\langle \hat{f}_i \rangle$	average fugacity across the membrane,	Pa
J	flux,	mol h^{-1} m^{-2}
l	membrane thickness, m	
L	phenomenological coefficient in eq. (2),	J^{-1} m^{-1} s^{-1}
NC	number of components in the solution fed to the module, dimensionless	(-)
n_f	number of fibres in a module, dimensionless	(-)
P	pressure,	Pa
P_m	permeability,	mol h^{-1} m^{-1}
R	universal gas constant,	8.314 J mol^{-1} K^{-1}
T	temperature,	K
V	liquid molar volume,	m^3 mol^{-1}
V_f	feed volumetric flow rate,	L h^{-1}
x	molar fraction in the liquid phase, dimensionless	(-)
y	molar fraction in the vapour phase, dimensionless	(-)

Subscript

i	component i	(-)

Superscripts

‘	feed/membrane interface	(-)
‘‘	membrane/permeate interface	(-)
i	component i	(-)
F	feed side	(-)
P	permeate side	(-)
L	liquid phase	(-)
V	vapour phase	(-)
PV	pervaporation	(-)
VP	vapour permeation	(-)
sat	saturation	(-)
R	retentate	(-)

Greek Symbols

μ	chemical potential,	J mol^{-1}
Λ	phenomenological coefficient defined by Eq. (6),	mol h^{-1} Pa^{-1} m^{-2}
γ	activity coefficient, dimensionless	(-)
γ^{∞}	infinite dilution activity coefficient, dimensionless	(-)
ϕ	fugacity coefficient of pure	

	component, dimensionless	(-)
$\hat{\phi}$	fugacity coefficient in solution, dimensionless	(-)
η	dynamic viscosity,	Pa s
ρ	density,	kg m^{-3}

REFERENCES

Baudot, A., Souchon, I. and Marin, M., Total Permeate Pressure Influence on the Selectivity of the Pervaporation of Aroma Compounds, Journal of Membrane Science, 158, 167 (1999).

Bengtsson, E., Trägardh, G. and Hallström, B., Concentration Polarisation during the Enrichment of Aroma Compounds from a Water Solution by Pervaporation, Journal of Food Engineering, 19, No. 4, 399 (1993).

Bird, R.B., Stewart, W.E. and Lightfoot, E.N., Transport Phenomena. John Wiley & Sons, Singapore (1960).

Blume, I., Schwering, P.J.F., Mulder, M.H.V. and Smolders, C.A., Vapour Sorption and Permeation Properties of Polydimethylsiloxane Films, Journal of Membrane Science, 61, 85 (1991).

Bomben, J.L., Bruin, S., Thijssen, H.A.C. and Merson, R.L., Aroma Recovery and Retention in Concentration and Drying of Foods, Advances in Food Research, 20, 1 (1973).

Bruining, W.J., A General Description of Flows and Pressures in Hollow Fiber Membrane Modules, Chemical Engineering Science, 44, No. 6, 1441 (1989).

Clément, R., Bendjama, Z., Nguyen, Q.T. and Néel, J., Extraction of Organics from Aqueous Solutions by Pervaporation: A Novel Method for Membrane Characterisation and Process Design in Ethyl Acetate Separation, Journal of Membrane Science, 66, 193 (1992).

Cussler, E.L., Diffusion: Mass Transfer in Fluid Systems, Cambridge University Press, New York (1984).

Deng, S., Sourirajan, A., Matsuura, T. and Farnand, B., Study of Volatile Hydrocarbon Emission Control by an Aromatic Poly(ether imide) Membrane, Industrial and Engineering Chemistry Research, 34, 4494 (1995).

Feng, X. and Huang, R.Y.M., Concentration Polarisation in Pervaporation Separation Processes, Journal of Membrane Science, 92, No. 3, p. 201 (1994).

Fleming, H.L. and Slater, C.S., Pervaporation. In: Winston, W.S. and Sirkar, K.K. (Eds.), Membrane Handbook, Van Nostrand Reinhold, New York, 103 (1992).

Fouda, A., Bai, J., Zhang, S.Q., Kutowy, O. and Matsuura, T., Membrane Separation of Low Volatile Organic Compounds by Pervaporation and Vapour Permeation, Desalination, 90, No. 1-3, 209 (1993).

Gales, L., Mendes, A. and Costa, C., Removal of Acetone, Ethyl Acetate and Ethanol Vapours from Air using a Hollow-fiber PDMS Membrane Module, Journal of Membrane Science, 197, 211 (2002).

Karlsson, H.O.E. and Trägardh, G., Heat Transfer in Pervaporation, Journal of Membrane Science, 119, 295 (1996).

Karlsson, H.O.E. and Trägardh, G., Pervaporation of Dilute Organic-water Mixtures: A Literature Review on Modelling Studies and Applications to Aroma Compound Recovery, Journal of Membrane Science, 76, No. 1-2, 121 (1993).

Kimmerle, K., Bell, C.M., Gudernatsch, W. and Chmiel, H., Solvent Recovery from Air, Journal of Membrane Science, 36, 477 (1988).

Lahiere, R.J., Hellums, M.W., Wijams, J.G. and Kaschemekat, J., Membrane Vapour Separation: Recovery of Vinyl Chloride Monomer from PVC Reactor Vents, Industrial and Engineering Chemistry Research, 32, 2236 (1993).

Leemann, M., Eigenberger, G. and Strathmann, H., Vapour Permeation for the Recovery of Organic Solvents from Waste Air Streams: Separation Capacities and Process Optimisation, Journal of Membrane Science, 113**,** No. 2, 313 (1996).

Ohlrogge, K., Peinemann, K.-V., Wind, J. and Behling, R.–D., The Separation of Hydrocarbon Vapours with Membranes, Separation Science and Technology, 25, No. 13-15, 1375 (1990).

Olsson, J. and Trägardh, G., Influence of Feed Flow Velocity on Pervaporative Aroma Recovery from a Model Solution of Apple Juice Aroma Compounds, Journal of Food Engineering, 39, 107 (1999).

Paul, H., Philipsen, C., Gerner, F.J. and Strathmann, H., Removal of Organic Vapours from Air by Selective Membrane Permeation, Journal of Membrane Science, 36, 363 (1988).

Pereira, C.C., Rufino, J.M., Habert, A.C., Nobrega, R., Cabral, L.M.C. and Borges, C.P., Membrane for Processing Tropical Fruit Juice, Desalination, 148, 57 (2002).

Ramteke, R.S., Singh, N.I., Rekha, M.N. and Eipeson, W.E., Methods for Concentration of Fruit Juices: A Critical Evaluation, Journal of

Food Science and Technology, 30, No. 6, 391 (1993).

Reid, R.C., Prausnitz, J.M. and Poling, B.E., The Properties of Gases and Liquids, 4th ed, McGraw-Hill, New York (1987).

Sampranpiboon, P., Jiraratananon, R., Uttapap, D., Feng, X. and Huang, R.Y.M., Separation of Aroma Compounds from Aqueous Solutions by Pervaporation Using Polyoctylmethylsiloxane (POMS) and Polydimethylsiloxane (PDMS) Membranes, Journal of Membrane Science, 174, 55 (2000).

Sancho, M.F.; Rao, M.A. and Downing, D.L., Infinite Dilution Activity Coefficients of Apple Juice Aroma Compounds, Journal of Food Engineering, 34, 145 (1997).

Sander, U. and Janssen, H., Industrial Application of Vapour Permeation, Journal of Membrane Science, 61, 113 (1991).

Shepherd, A.G., Projeto, Construção e Avaliação de Módulos de Fibras-ocas para Recuperação, por Pervaporação, de Aromas do Suco de Laranja. Master's Thesis, Federal University of Rio de Janeiro, Brazil (2000).

Shepherd, A.G., Habert, A.C. and Borges, C.P., Hollow-fibre Modules for Orange Juice Aroma Recovery Using Pervaporation, Desalination, 148, 111 (2002).

Smith, J.M. and Van Ness, H.C., Introduction to Chemical Engineering Thermodynamics, 4th ed., McGraw-Hill, New York (1987).

Uchytil, P. and Petrickovic, R., Vapour Permeation and Pervaporation of Propan-1-ol and Propan-2-ol in Polyethylene Membrane, Journal of Membrane Science, 209, No. 1, 67 (2002).

Wijmans, J.G. and Baker, R.W., The Solution-diffusion Model: A Review, Journal of Membrane Science, 107 No. 1-2, 1 (1995).

Yeom, C.K., Lee, S.H., Song, H.Y. and Lee, J.M., Vapour Permeation of a Series of VOCs/N_2 Mixtures through PDMS Membrane, Journal of Membrane Science, 198, No. 1, 129 (2002).